

Düzce University
Journal of Science & Technology

https://dergipark.org.tr/tr/pub/dubited

Research paper

Rogowski Coils with Nickel Alloy Flexible Core and Peroformance Comparisons

Gizem Merve Aydın[a], *Emin Yıldırız*[b,*]

[a]Sakarya Electricity Distribution Inc., Sakarya, Türkiye.
[b]Düzce University, Faculty of Engineering, Department of Electric and Electronics Engineering, Düzce, Türkiye.
[*]**Corresponding author:** eminyildiriz@duzce.edu.tr

Article information:
Received: 03/03/2025, Revision: 25/07/2025, Accepted: 07/08/2025
DOI: 10.29130/dubited.1650136

ABSTRACT

The instantaneous currents must be measured precisely and accurately in order to monitor electrical circuits under different operating conditions. Rogowski Coils (RC) can be easily connected even in narrow spaces where the measuring device cannot enter. They perform current measurement using the secondary voltages produced at a few mV levels even at the nominal currents (3000 - 60000 A). Therefore, it is difficult to make measurements with RCs, especially at low current values such as a few ten amperes, and the results are prone to the measurement errors. In order to increase the measurement sensitivity without changing the physical dimensions of the RC, a magnetic-core structure can be preferred instead of an air-core. In this paper, the magnetic filaments have been produced using nickel alloys at different ratios (40% and 60%). Flexible magnetic-core RCs have been developed by winding the magnetic filaments. Considering the flexibility of the core, the magnetic filaments have been produced in two different alloy ratios. The relative permeabilities of the developed magnetic filaments have been determined by experimental studies and their linear characteristics in the range of 5-400 A have been verified by finite element analysis.

Keywords: *Rogowski Coil, Flexible Magnetic Core, Current Measurement*

I. INTRODUCTION

It is very important to measure the currents accurately and precisely for the traceability of an AC electrical systems. The steady-state currents are not always measured at 50/60 Hz frequencies. Current transformers (Yu et al., 2006; Shang et al., 2012), Hall effect sensors (Crescentini et al., 2021; Chen & Chen, 2010) or RCs (Nanyan et al., 2018; Shepard et al., 2000; Shafiq et al., 2022; Liu et al., 2010) are preferred for measuring high currents. The secondary winding outputs of the current transformer are connected to an ampermeter and measure the sinusoidal currents at 50/60 Hz frequencies. Thus, the high currents in the primary-side are reduced to measurable current levels on the secondary-side. The secondary of the current transformer is connected to a device with a small internal resistance, it works like a short-circuit and if the core operates below the saturation region, it can perform a linear measurement. However, measurement errors may occur in the conventional current transformers in case of distorted waveforms such as currents above the rated current, short circuits, non-linear loads, and transient events such as switching (Anigi et al., 2012). For the current transformers defined in four different accuracy classes according to TS 620 EN 60044-1, the largest current error accepted at 120% of the rated current is 1% (Çınar et al., 2016). Since the conventional air-core RCs exhibit a linear magnetic property, they can measure very small currents to very high currents with the same accuracy with the right integrator designs (Samimi et al., 2014).

Cite as: Aydın, G. M. & Yıldırız, E. (2025). Rogowski coils with nickel alloy flexible core and performance comparisons. *Düzce University Journal of Science and Technology*, *13*(4), 1601-1611.

Depending on the operating conditions, it may be necessary to measure pulse currents at high frequencies. The current measurement is also necessary for monitoring transient events at the switching moments or to examine the system designs and safe operating conditions. RC can also provide a meaningful output signal under all these operating conditions.

The RC output signal is on the order of a few mV for nominal primary currents at frequencies of 50/60 Hz. The integrators are used at the RC output to obtain a measurable primary current level by scaling it (Shi et al., 2020; Bawankule et al., 2022). When the sensor output is low, the integrator design must be very precise. Otherwise, the sensing gain at the integrator output may be too low, or distorted signals may be observed on the output waveform. Therefore, it is preferable to have high signal levels at the output of RCs.

In recent years, the researchers have been investigating the performance and design limits of RCs in the unusual applications where they have not been used before. PCB-based RCs proposed for measuring currents in high-frequency switching elements are the most current RC designs (Zhang et al., 2021, Xin et al., 2025). PCB-based RCs can be either fully enclosed or clip-on (Bawankule et al., 2025). Various winding designs and connection patterns have also been proposed for them (Ranasingh et al., 2022; Zhan et al., 2024). The conventional RCs, by their operating principle, measure high-amplitude pulse currents. On the other hand, PCB-based RCs are designed for high frequencies, with low winding counts, small sizes, and they are not flexible. Flexible RC design proposals with high measurement accuracy represent a significant gap in the literature that needs to be explored.

The RCs are air-core current meters and operate on the basis of Ampere and Faraday's laws. Air-core RCs can measure the currents with distorted waveforms, high frequencies (Dubickas & Edin, 2007) and switching states (Kang et al., 2023). Since they do not have a magnetic core, they do not experience saturation problems and can measure currents from a few A to a few kA with their linear characteristics. Despite these advantages, it is relatively difficult to measure low-level currents with air-core RCs. In recent years, the researchers have suggested magnetic alloy composite cores to increase the measurement accuracy of traditional RCs. In (Marracci et al., 2017), the use of a rectangular cross-section solid composite core produced in PLA using Fe_3O_4 in a commercial 3D printer in an RC core has been suggested. With the composite core produced with a 3D printer, a linear magnetic characteristic has been obtained and low current values could be measured accurately. However, the use of solid core eliminates the flexibility that is the biggest advantage of air-core RCs. The use of silicone rubber to provide flexibility to the composite magnetic core has been suggested in (Wei et al., 2020). By mixing MnZn-Ferite particles and silicone rubber in different ratios, a flexible core with 18 times higher magnetic permeability than the air-core RC has been produced. However, the experimental performance results of the RC with the flexible core have not been shared. The starting point of the research that is the subject of this paper has been this gap in the literature. Flexible magnetic cores can be obtained by combining silicon, rubber, or plastic with powdered ferromagnetic elements. These ferromagnetic elements can be magnetite (Fe_2O_4), iron powder, nickel, cobalt, etc. The relative magnetic permeabilities of ferromagnetic elements are affected by operating frequency and ambient conditions such as temperature. According to (Timsit et al., 2008), the relative permeability of nickel is around 160 up to approximately 300 kHz. In (Pozo et al., 2019), the relative permeabilities of the conventional ferromagnetic materials are compared. Although the comparison frequency is not specified, the magnetic permeabilities of Fe3O4 Nickel and Cobalt are given as 100, 600 and 250, respectively. The magnetic permeabilities of elements such as nanocrystalline and MnZn ferrite, used in EMI filters, exceed 1000 up to 100 kHz (Takahashi et al., 2019). However, these alloys are difficult to obtain in powder form. To ensure homogeneous production when selecting ferromagnetic elements, powder particles as small as possible should be used. In this study, nickel was chosen for flexible magnetic core production due to its ease of supply and cost-effectiveness in very small powder form. Furthermore, nickel has more corrosion resistant than other elements.

In this study, flexible ferromagnetic filaments were produced using a PLA+nickel alloy in a filament extrusion machine. These filaments were directly used to develop toroidal RC ferromagnetic cores. The design and manufacturing processes of the proposed RC have been described in the second section of this manuscript. Experimental studies conducted between 60A and 400A have been presented in the third section, and FEA models and analysis results supported by experimental studies have been disclosed in the fourth section. The findings and recommendations for future work are evaluated in the Conclusion. The novelties that this paper has added to the literature can be listed item by item as follows:

- Proposing new RC core structures that are flexible like conventional RCs but have higher magnetic permeability.
- Investigation of the linear characteristics of nickel alloy flexible magnetic cores through experimental and FEA analyses.
- The effect of different nickel alloy ratios on the output signal of flexible magnetic-core RCs.

II. DESIGN AND PRODUCTION OF FLEXIBLE RC

The inner and outer diameters and the cross-section area of the RC are the most important parameters in the RC design. In this paper, while determining the design parameters, the RCT16 model of ACCUENERGY, a commercial product, has been taken as the reference model (Accuenergy, 2025). Accordingly, the dimensions of the developed RC are shown in Table 1.

Table 1. Properties of the commercial RC taken as reference model.

Current Range (A)	Inner Diameter (m)	Outer Diameter (m)	Cross Section (mm^2)	Length (m)
5-200	1,06	1,43	0,97	0,4

The inductance calculations are related to the dimensions and the cross-sectional area of the coil for a conventional air-core RC (Hlavacek et al., 2008). The cross-sectional area of the conventional RC can be circular, rectangular, elliptical, etc. (Hlavacek et al., 2008; Wang et al., 2024; Al-Sowayan, 2014). In a circular cross-section RC, the self-inductance calculation of the secondary winding is given in Eq. (1) and the mutual inductance calculation is given in Eq. (2). In these equations, a and b represent the inner diameter and outer diameter of RC, respectively. μ is the magnetic permeability in the cross-sectional area of RC. The self-inductance of a winding is the ratio of the flux linkage to the current passing through it. For the calculation of mutual inductance, the relationship between the flux linkage that the current passing through the opposite winding passes through the other winding must be known. The calculation of the mutual inductance between the primary and secondary sides is given in Eq. (3). Here, λ_{12} represents the flux linkage created by the primary current through the RC, and I_1 represents the primary current. The magnetic flux created by the primary current and passing through RC must be known in order to calculate the magnetic flux linkage in Eq. (4). As the magnetic permeability of the region through which the magnetic flux passes changes, the amount of flux taken into account in the inductance calculations will also change. The voltage induced on the RC by the primary current is related to the mutual flux linkage. Therefore, the magnetic permeability of the RC is also important as well as its dimensions in the RC design.

$$L_2 = \frac{\mu {N_2}^2}{2}\left(a + b - 2\sqrt{ab}\right) \quad (1)$$

$$M_{21} = \frac{\mu N_2}{2}\left(a + b - 2\sqrt{ab}\right) \quad (2)$$

$$M_{21} = \frac{\lambda_{12}}{I_1} \quad (3)$$

$$\lambda_{12} = N_2 \varphi_{12} \quad (4)$$

The 3D model and the cross-sectional area of the designed RC with flexible-core are given in Figure 1. Flexible filaments produced in different alloys are wound inside the flexible case of the conventional RC, which is hollow. Thus, as seen in Figure 1, the cross-sectional area of the RC consists of a plastic protective sheath, flexible nickel alloy magnetic filaments and air-gap. The presence of nickel alloy filaments in the inner cavity of the plastic sheath will increase the total magnetic flux density in the RC cross-sectional area.

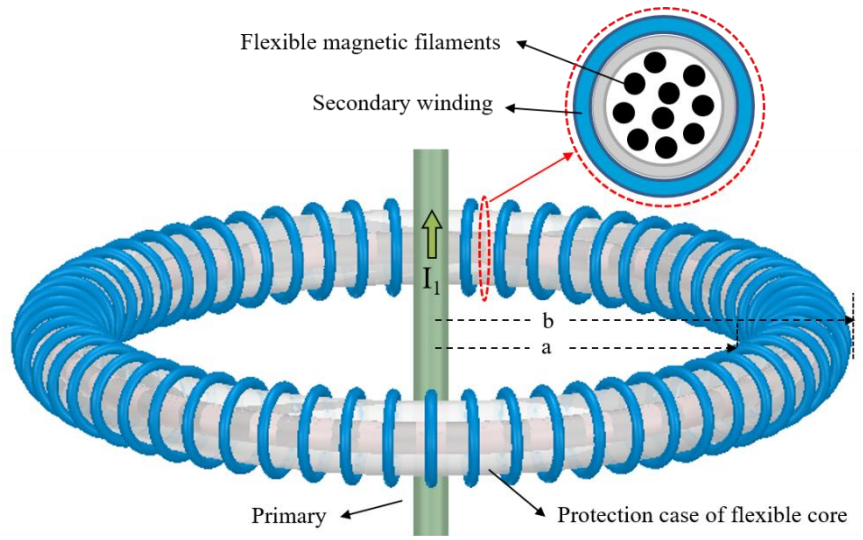


Figure 1. The RCs with flexible-core.

The production processes are shown in Figure 2. In the first stage, the filaments have been produced with different alloy ratios using nickel particles smaller than 5 µm with 99.5% purity and TPU polymer with 80A Shore hardness. A single screw extruder with a 2 mm output head has been used for the filament production. The filaments with a fixed diameter of 1.75 mm have been obtained by stretching from the extruder outlet. To ensure consistent filament dimensions and flexibility through a proper stretching process, the nickel alloy ratio in the production process is set between 40% and 60%. Above 60% nickel, flexibility decreases and breakage during stretching can occur. Before production, both polymer and fillers have been dried in a vacuum oven at 80 °C for 6 hours. The produced nickel alloy filaments have been wrapped in a plastic sheath cut to fit the dimensions of the commercial RC model taken as reference. Then, 825 windings of 0.4 mm diameter H type winding wire have been wound on the plastic sheath at equal intervals and smoothly. In order to reduce the effect of external noise on the RC, shielding is done using 14 micron thick aluminum foil with two layers on the secondary windings. In this paper, in order to fully demonstrate the effect of nickel alloy filaments on the RC performance, three identical sized and wound RCs have been produced, namely 40% nickel filament, 60% nickel filament and without filament (air-core).



Figure 2. The production of the RCs with flexible-core.

III. EXPERIMENTAL RESULTS

A transformer with a ratio of 50:1 has been used to test the developed RCs in the laboratory environment. Thus, the primary currents up to 400A have been obtained. The experimental setup is shown in Figure 3. The primary-side is formed as an 8-winding conductor, taking into account the output current level of the adj. power supply. Thus, the primary current has been increased in 5A increments and the RC output voltages have been measured. The effective value of the secondary voltage of the RC has been measured with a 2-channel 100 MHz oscilloscope. The primary current passing through RC has also been measured with a calibrated clamp meter at each stage of the experimental measurements. Table 2 shows the voltages measured at the secondary-side of RCs developed at some primary currents.

Table 2. Test results of the investigated RCs.

Primary Current (A)	**Secondary Voltage (mV)**		
	Air-Core	**40% Nickel Alloy**	**60%Nickel Alloy**
60,2	6,4	7,6	7,9
100,2	10,2	12,7	13,7
200,5	19,7	24,4	26,2
300,4	29,7	35,9	37,9
400,7	39,5	49,9	52,6

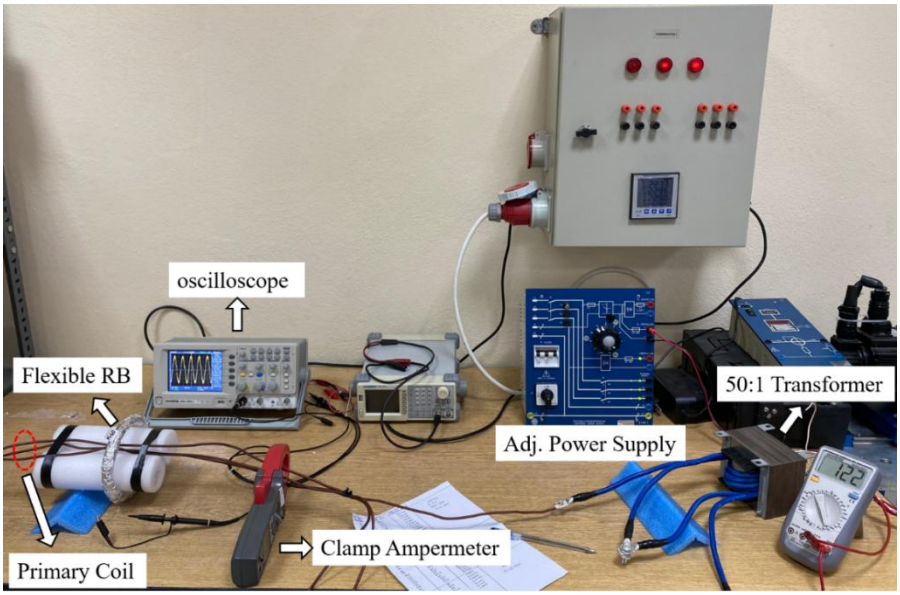


Figure 3. The test setup used for the measurements.

IV. FINITE ELEMENT METHOD AND ANAYSIS OF RC

The amount of magnetic flux passing through the inner cross-sectional area of RC should be analyzed separately for each type of the material (Figure 1). The total magnetic flux φ_T is shown as Eq. (5). The voltage induced on a RC can be calculated with Eq. (6). There are three different magnetic materials in the cross-sectional area of the RC. These are outer plastic protection sheath, nickel alloy filaments and air. The relative magnetic permeability of air and the plastic protection sheath is assumed to be identical and equals to one to simplify the calculation. Since modeling each of the 1.75 mm diameter filaments in 3D FEA would increase the analysis time, an equivalent cross-sectional area has been defined for the total cross-section area of the filaments (Figure 4). φ_1 is the flux passing through the plastic sheath and air-gap. The cross-sectional area defined in the middle of RC is used to define the fluxes passing through the nickel alloy filaments, and has been shown as φ_2. Thus, the total magnetic flux has been defined by two regions with two different permeabilities. The relative magnetic permeabilities or B-H curves of the materials used must be known for a realistic FEA model. In this paper, the magnetic permeabilities of 40% and 60% nickel alloy filaments have been calculated using the experimental results. Experimental studies have been carried out from 5 A to 400A primary current. Figure 5 shows the calculated B-H curves of the produced filaments. The

magnetic field intensity H in the curve is found from Ampere's law using the current applied to the primary and the average core path of the RC. The magnetic flux density B is calculated using Faraday's law using the number of secondary turns, the cross-sectional area of the RC core, and the secondary voltage measured by the scope.

$$\varphi_T = \varphi_1 + \varphi_2 \quad (5)$$

$$e_2 = N_2 \frac{d\varphi_T}{dt} \quad (6)$$

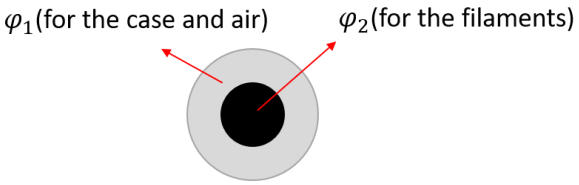
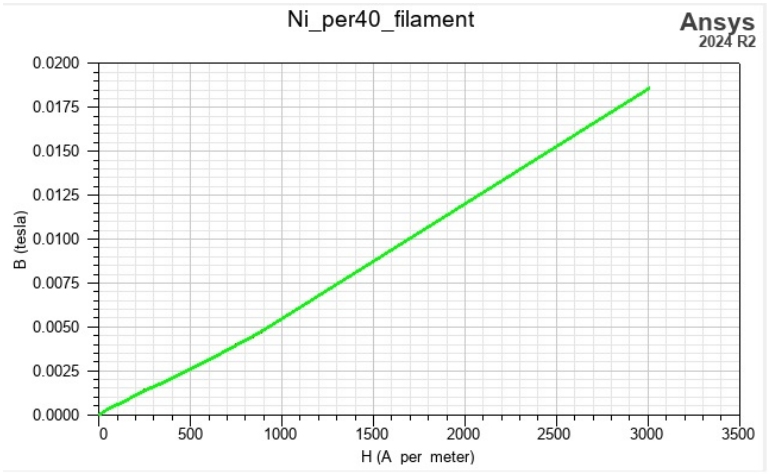
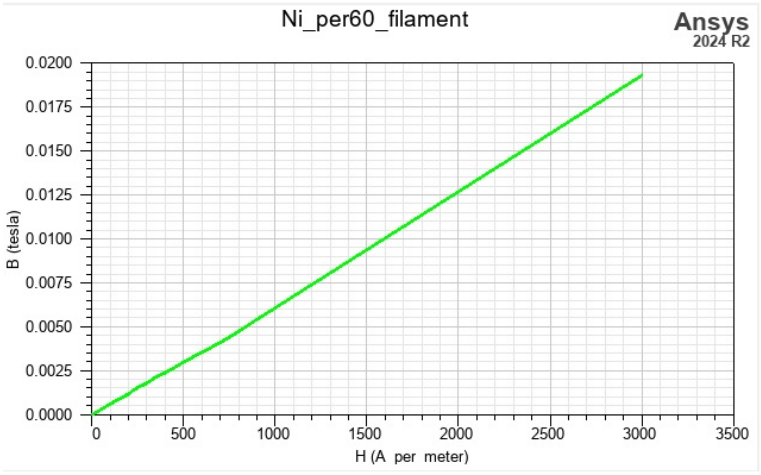


Figure 4. The cross-sectional areas and fluxes of the developed RCs in the FEA model.



(a)

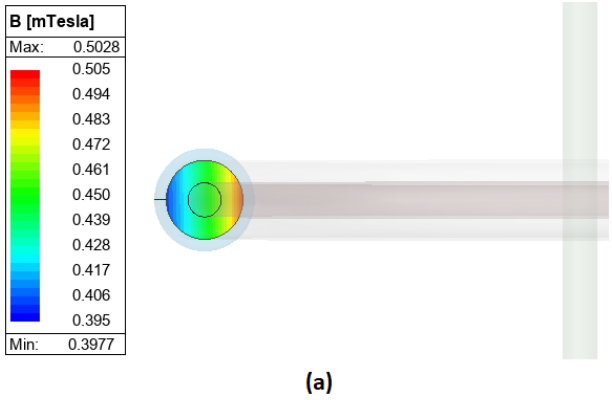


(b)

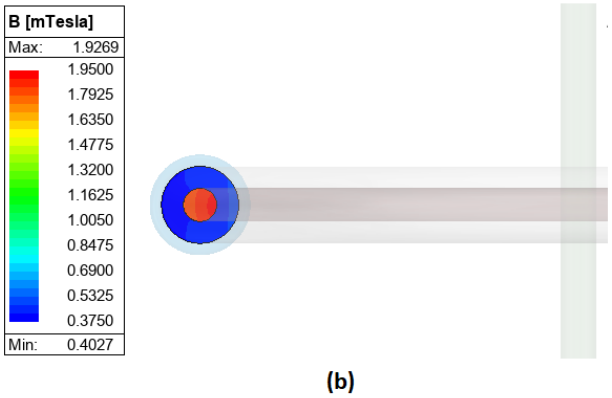
Figure 5. B-H curves of nickel alloy filaments (a) 40% nickel alloy and (b) 60% nickel alloy.

The FEA models of the developed flexible magnetic core RCs have been created based on their actual dimensions. Considering the relative magnetic permeabilities obtained with the experimental results, the

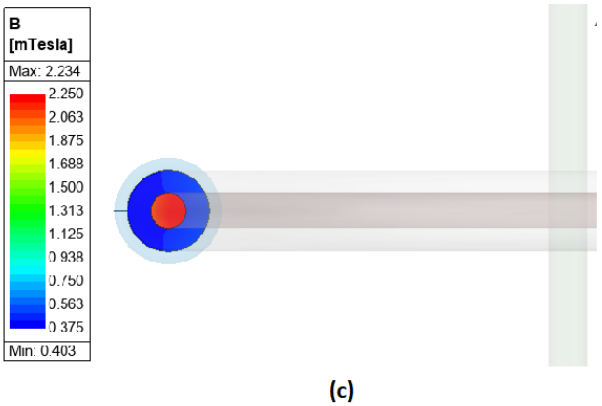
magnetic flux densities created by the 100 A primary current in the cross-sectional area of the RCs are given in Figure 6. When the ratio of nickel alloy is 60%, the magnetic flux density on the filament sections has reached up to 2.81 mT. The magnetic flux density in the 40% nickel alloy filament section is at most 1.253 mT at the same primary current. It is clearly seen that the magnetic flux density increases as the ratio of nickel alloy increases. Since the magnetic permeability of the filaments is higher than that of air, it is seen that the magnetic fluxes are concentrated in the center of the cross-sectional area. Since there is no ferromagnetic material in the air-core RC, the maximum flux density within the cross-sectional area of the RC is up to 0.5 mT. Also, as the distance from the primary conductor increases, the magnetic flux density in the section of the air-core RC decreases linearly and smoothly depending on the distance.



(a)



(b)



(c)

Figure 6. Magnetic flux densities in the cross-sectional areas of the developed RCs at 100A primary current (a) Air-core, (b) 40% nickel alloy and (c) 60% nickel alloy.

The magnetic flux passing through the cross-sectional area will also increase as the primary current increases. In Figure 7, the measurement and FEA analysis results for the primary currents between 5A and 400A are given together. In the FEA model of the air-core RC, the relative permeability of all flux regions is equals to one. When the FEA analysis results are examined, it is seen that the output voltage of RCs increases

linearly as the primary current increases for all of the RC designs. Focusing on the low primary currents, it is seen that RCs using nickel alloy filaments give higher output voltages than the air-core RC results in both experimental and FEA analysis results. The FEA analyses are consistent with the experimental results since the BH curves of the filaments have been obtained using these results. This consistency proves the reality of the developed FEA model and the success of the solution mesh.

On the other hand, the FEA results of the air-core RC are lower than the experimental results. Depending on the magnitude of the primary current, the error between experimental and FEA results varies between 14.41% and 18.09%.There are likely several reasons for this error. Firstly, the 3D FEA model of the flexible air-core RC has been obtained with perfect symmetry. However, the perfect production is not possible in the experimental RC. Even the angle between the turns and density of the secondary windings affect the measurement performance of the RC (Han et al., 2015). In summary, the manufacturing tolerances are the main reason for this error. The second important reason for the difference between the experimental and FEA result of the air-core RC is that, to simplify the model, the magnetic permeability of all cross-sections other than the filament is assumed to be equal to the gap. This assumption is not very effective in nickel alloy flexible-core RCs. The magnetic permeability of nickel alloy filaments is considerably higher than the relative magnetic permeability of air and the plastic sheath. However, in the air-core RC, the magnetic permeability of the plastic sheath is similar to that of air, and only slightly higher (Prince et al., 2021; Zárybnická et al., 2023). Furthermore, since there is no ferromagnetic effect that concentrates the magnetic flux in the air-core RC, the magnetic flux densities are very low. Therefore, the adaptive mesh accuracy generated in the FEA analysis is not high. Another reason is that although a single primary conductor is placed at the center of a fully circular RC in the FEA analysis, the experimental positioning and conditions are somewhat different. Due to these differences, the FEA analysis results of the air-core RC differ slightly from the experimental results. When all the experimental and the FEA analysis results are evaluated, the linearity of all the RCs is proven for the observed primary current range.

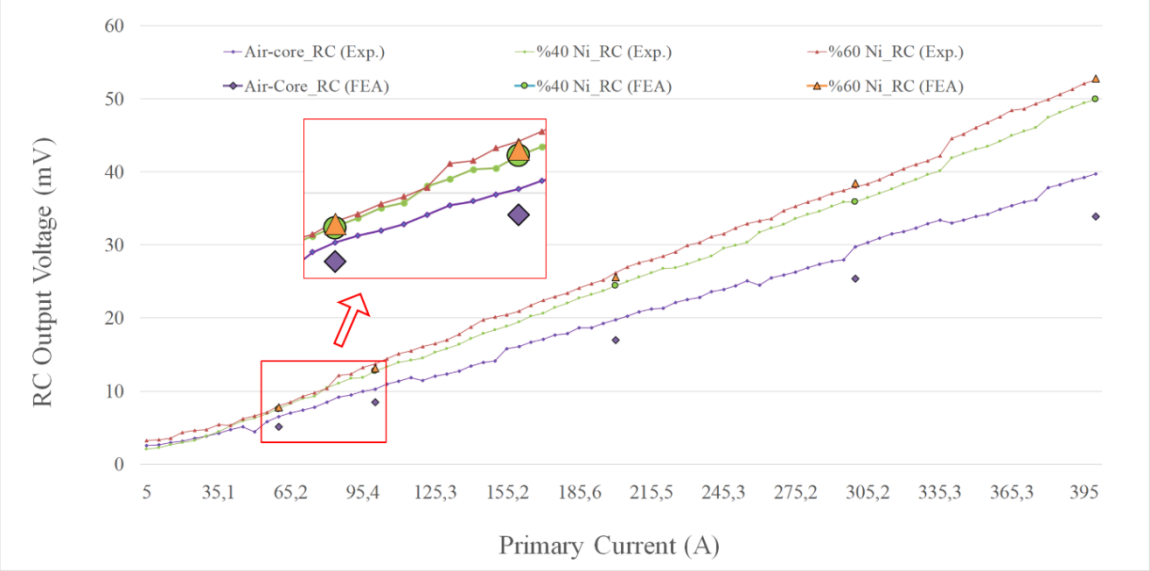


Figure 7. According to FEA and experimental measurements, the changes in output voltages of the RCs.

V. CONCLUSION

In this paper, the RCs with flexible magnetic core have been developed using the filaments containing 40% and 60% nickel alloy. The output voltages of the developed RCs have been measured in the range of 5-400A primary current and the results have been compared with the air-core RC with the same properties. Nickel alloy RCs give higher output voltages at the same primary current. The strengthening of the output signal of RC will mean an increase in the measurement sensitivity. Thus, the flexible magnetic-core RCs developed can be easily used in control circuits and operating panels where the rated current values are relatively low and conventional current transformers are currently used. The B-H curves obtained from the experimental results have been used in the 3D FEA analyses and the obtained results have been presented comparatively for all the RC models. Nevertheless, the experimental and FEA results confirmed the linearity of the developed nickel alloy flexible core RCs. It is observed that the output voltage of the RC increases as the ratio of nickel alloy increases. However, due to the stretching process and flexibility constraints involved

in the production of ferromagnetic filaments, nickel alloy ratios have been tested at up to 60% in experimental studies. This ratio can be increased by exploring flexible filament production methods. With this inference, stronger RC output signals can be obtained by increasing the ratio of magnetic powders such as nickel or Fe2O4 in the alloy within the flexibility limits.

By examining the effects of external environmental factors such as temperature and corrosion on the flexible magnetic-core RCs under different operating conditions, the RCs suitable for commercialization can be developed.

DECLARATIONS

Acknowledgements: This work is supported by Düzce University Scientific Project (Project no: 2022.06.03.1349). The authors thank Düzce University for their support.

Author Contributions: The authors' contributions to this study are as follows: Conceptualization, E.Y.; Methodology, E.Y. and G.M.A.; Validation, E.Y. and G.M.A.; Investigation, E.Y. and G.M.A.; Resources, G.M.A.; Data Curation, G.M.A.; Writing—Original Draft, E.Y.; Writing—Review & Editing, E.Y.; Supervision, E.Y. All authors have read and approved the final version of the manuscript.

Conflict of Interest Disclosure: The author/authors declare no conflict of interest.

Copyright Statement: The authors retain the copyright of their work published in the journal, which is licensed under the CC BY-NC 4.0 license, allowing others to share and adapt the work for non-commercial purposes with appropriate attribution.

Funding/Supporting Organizations: This research received no external funding.

Ethical Approval and Participant Consent: This study does not involve human or animal participants. All procedures followed scientific and ethical principles, and all referenced studies are appropriately cited.

Plagiarism Statement: This article has been evaluated for plagiarism and no instances of plagiarism were detected.

Availability of Data and Materials: Data sharing is not applicable to this study.

Use of AI Tools: The authors declare that no Artificial Intelligence (AI) tools were used in the creation of this article.

REFERENCES

Accuenergy. (2025, February 25). *AcuCT Flex Series Rogowski Coil CT datasheet*. https://accucdn.accuenergy.com/wp-content/uploads/acuct-flex-series-rogowski-coil-ct-datasheet.pdf

Al-Sowayan, S. (2014). Improved mutual inductance of Rogowski coil using hexagonal core. *World Academy of Science, Engineering and Technology International Journal of Electrical, Computer, Energetic, Electronic and Communication Engineering, 8(2),* 293-296.

Anigi, E., Karacasu, Ö., & Hocaoğlu, M. H. (2012, November 29 – December 1). Ölçü akım transformatörlerinin doğruluğunun sinüzoidal olmayan şartlar altında deneysel incelenmesi, In *Proceedings of ELECO 2012 Elektrik - Elektronik ve Bilgisayar Mühendisliği Sempozyumu* (pp. 148-152). Bursa Türkiye.

Bawankule, P., & Chandrasekaran, K. (2022, October 7-9). Rogowski coil with an active integrator for impulse current measurement. *In Proceedings of the 2022 IEEE 3rd Global Conference for Advancement in Technology (GCAT)* (pp. 1–6). Bangalore, India.

Bawankule, P., & Chandrasekaran, K. (2025, January 20-22). Analyzing the Performance of 3D PCB Rogowski Coil in Pulsed Current Measurement Using Finite Element Method. *In Proceedings of the 2025 Fourth International Conference on Power, Control and Computing Technologies (ICPC2T)* (pp. 1–6). Raipur, India, https://doi.org/10.1109/ICPC2T63847.2025.10958704

Chen, K. L., & Chen, N. (2010). A new method for power current measurement using a coreless Hall effect current transformer. *IEEE Transactions on Instrumentation and Measurement, 60*(1), 158-169. https://doi.org/10.1109/TIM.2010.2049234

Crescentini, M., Syeda, S. F., & Gibiino, G. P. (2021). Hall-effect current sensors: Principles of operation and implementation techniques. *IEEE Sensors Journal, 22*(11), 10137-10151. https://doi.org/10.1109/JSEN.2021.3119766

Çınar, H., İmal, N., & Şener, E. (2016). Akım ölçü transformatörleri çalışma bölgesi analizi. *Düzce Üniversitesi Bilim ve Teknoloji Dergisi, 4*(2), 782-790.

Dubickas, V., & Edin, H. (2007). High-frequency model of the Rogowski coil with a small number of turns. *IEEE Transactions on Instrumentation and Measurement, 56*(6), 2284-2288. https://doi.org/10.1109/TIM.2007.907965

Han, R. Y., Wu, J. W., Ding, W. D., Jing, Y., Zhou, H. B., Liu, Q. J., & Qiu, A. C. (2015). Hybrid PCB Rogowski coil for measurement of nanosecond-risetime pulsed current. *IEEE Transactions on Plasma Science, 43*(10), 3555-3561. https://doi.org/10.1109/TPS.2015.2415517

Hlavacek, J., Prochazka, R., Draxler, K., & Kvasnicka, V. (2008, September 22-24). The Rogowski coil design software. In *Proceedings of the16th IMEKO TC4 International Symposium.* Florence, Italy.

Kang, J., Zhu, A., Chen, Y., Luo, H., Yao, L., & Xin, Z. (2023). An online gate oxide degradation monitoring method for SiC MOSFETs with contactless PCB Rogowski coil approach. *IEEE Transactions on Power Electronics, 38*(8), 9673-9684. https://doi.org/10.1109/TPEL.2023.3270820

Liu, Y., Lin, F., Zhang, Q., & Zhong, H. (2010). Design and construction of a Rogowski coil for measuring wide pulsed current. *IEEE Sensors Journal, 11*(1), 123-130. https://doi.org/10.1109/JSEN.2010.2052034

Marracci, M., Tellini, B., & Bertolucci, E. (2017, May). Study and characterization of a Rogowski coil with superparamagnetic magnetite core. In *Proceedings of the 2017 IEEE International Instrumentation and Measurement Technology Conference (I2MTC),* Turin, Italy, https://doi.org/10.1109/I2MTC.2017.7969951

Nanyan, A. N., Isa, M., Hamid, H. A., Rohani, M. N. K., & Ismail, B. (2018). The Rogowski coil sensor in high current application: A review. *IOP Conference Series: Materials Science and Engineering, 318*(1), Article 012054. https://doi.org/10.1088/1757-899X/318/1/012054

Pozo, B., Garate, J. I., Araujo, J. A., & Ferreiro, S. (2019). Energy harvesting technologies and equivalent electronic structural models. *Electronics*, *8*(5), Article 486. https://doi.org/10.3390/electronics8050486

Prince, T. J., Riley, E. J., & Miller, S. W. (2021). Additive manufacturing of PLA-based microwave circuit-analog absorbers. *IEEE Transactions on Electromagnetic Compatibility, 63*(5), 1341-1346. https://doi.org/10.1109/TEMC.2020.3044014

Ranasingh, S., Pradhan, T., & Raju, D. K. (2022). Contactless current sensor with novel coil designs and Hall-effect based electron device for dynamic precision adjustment. *IEEE Sensors Journal, 22*(21), 20626-20634. https://doi.org/10.1109/JSEN.2022.3207276

Samimi, M. H., Mahari, A., Farahnakian, M. A., & Mohseni, H. (2014). The Rogowski coil principles and applications: A review. *IEEE Sensors Journal, 15*(2), 651-658. https://doi.org/10.1109/JSEN.2014.2362940

Shafiq, M., Stewart, B. G., Hussain, G. A., Hassan, W., Choudhary, M., & Palo, I. (2022). Design and applications of Rogowski coil sensors for power system measurements: A review. *Measurement, 203,* Article 112014. https://doi.org/10.1016/j.measurement.2022.112014

Shang, Y., Li, H., Wang, J., Wu, J., & He, X. (2012, May 28-31). Analysis and design of a current transformer fed power supply from high AC voltage cable*. In 2012 IEEE International Symposium on Industrial Electronics*, Hangzhou, China, https://doi.org/10.1109/ISIE.2012.6237080

Shepard, D. E., & Yauch, D. W. (2000). *An overview of Rogowski coil current sensing technology* (Technical report). *LEM High Current Systems.*

Shi, Y., Xin, Z., Loh, P. C., & Blaabjerg, F. (2020). A review of traditional helical to recent miniaturized printed circuit board Rogowski coils for power-electronic applications. *IEEE Transactions on Power Electronics, 35*(11), 12207-12222. https://doi.org/10.1109/TPEL.2020.2984055

Takahashi, S., Ogasawara, S., Takemoto, M., Orikawa, K., & Tamate, M. (2019, November 25-28). Experimental evaluation of the relationship between filter inductor impedances and dimensional resonances of MnZn ferrites. In *Proceedings of the 2019 IEEE 4th International Future Energy Electronics Conference (IFEEC)*, Singapore, https://doi.org/10.1109/IFEEC47410.2019.9015169.

Timsit, R. S. (2008). High speed electronic connector design: A review of electrical and electromagnetic properties of passive contact elements—part 1. *IEICE transactions on electronics*, *91*(8), 1178-1191. https://doi.org/10.1093/ietele/e91-c.8.1178

Wang, J., Wang, H., Mao, M., & Ma, X. (2024). Analysis and optimization of the stray capacitance of Rogowski coils. *Applied Sciences, 14*(17), Article 7748. https://doi.org/10.3390/app14177748

Wei, C., Lin, C., Boyang, M., Yuntao, G., & Shi, Y. (2020, October 18-21). Development of magnetic core framework for flexible Rogowski coil current transducer. In *Proceedings of IECON 2020 The 46th Annual Conference of the IEEE Industrial Electronics Society*, Singapore, https://doi.org/10.1109/IECON43393.2020.9254471

Xin, Z., Yao, Y., Kang, J., Li, Q., Zhou, Z., & Shi, Y. (2025). A closed-loop compensated Rogowski coil current sensor for three-phase inverter. *IEEE Transactions on Power Electronics. 40*(1), 2126-2138. https://doi.org/10.1109/TPEL.2024.3464121

Yu, H., Yuan, J., & Zou, J. (2006). Design of novel structure current transformer with shielding coils for overcoming the saturation of core. *IEEE Transactions on Magnetics, 42*(4), 1431-1434. https://doi.org/10.1109/TMAG.2006.872478

Zárybnická, L., Pagáč, M., Ševčík, R., Pokorný, J., & Marek, M. (2023). Effect of topology parameters on physical–mechanical properties of magnetic PLA 3D-printed structures. *Magnetochemistry, 9*(12), Article 232. https://doi.org/10.3390/magnetochemistry9120232

Zhan, Y., Feng, G., Wan, J., Li, X., Jin, R., Sun, P., Zhao, Z. & Cui, X. (2024). PCB Rogowski coil array with discrete electrostatic shielding for current measurement of paralleled chips in power devices. *IEEE Transactions on Power Electronics, 39*(8), 10276-10286. https://doi.org/10.1109/TPEL.2024.3392937

Zhang, W., Sohid, S. B., Wang, F., Cui, H., & Holzinger, B. (2021). High-bandwidth combinational Rogowski coil for SiC MOSFET power module. *IEEE Transactions on power electronics, 37*(4), 4397-4405. https://doi.org/10.1109/TPEL.2021.3127545